

# Journal of Materials Chemistry C

Accepted Manuscript



This article can be cited before page numbers have been issued, to do this please use: H. L. Lee, K. H. Lee and J. Y. Lee, *J. Mater. Chem. C*, 2019, DOI: 10.1039/C9TC00701F.



This is an Accepted Manuscript, which has been through the Royal Society of Chemistry peer review process and has been accepted for publication.

Accepted Manuscripts are published online shortly after acceptance, before technical editing, formatting and proof reading. Using this free service, authors can make their results available to the community, in citable form, before we publish the edited article. We will replace this Accepted Manuscript with the edited and formatted Advance Article as soon as it is available.

You can find more information about Accepted Manuscripts in the [author guidelines](#).

Please note that technical editing may introduce minor changes to the text and/or graphics, which may alter content. The journal's standard [Terms & Conditions](#) and the ethical guidelines, outlined in our [author and reviewer resource centre](#), still apply. In no event shall the Royal Society of Chemistry be held responsible for any errors or omissions in this Accepted Manuscript or any consequences arising from the use of any information it contains.

# Indoloindole as a new building block of hole transport type host for stable operation in the phosphorescent organic light-emitting diodes

Ha Lim Lee, Kyung Hyung Lee, Jun Yeob Lee\*

School of Chemical Engineering, Sungkyunkwan University  
2066, Seobu-ro, Jangan-gu, Suwon-si, Gyeonggi-do, 440-746, Korea

Fax: (+) 82-31-299-4716

E-mail: leej17@skku.edu

\* To whom correspondence should be addressed

## Abstract

An organic material for application as a p-type host of phosphorescent organic light-emitting diodes was newly developed using an indoloindole moiety as a hole transport unit. The indoloindole derived organic material showed better hole transport property than a common carbazole based organic material. The good hole transport property of the indoloindole derivative allowed the use of it as the p-type host material in the exciplex type mixed host of phosphorescent organic light-emitting diodes. The new host extended the lifetime of the yellow phosphorescent OLEDs by more than 10 times compared with a conventional p-type host while achieving the similar external quantum efficiency.

Key words : indoloindole, host, mixed host, efficiency

## Introduction

View Article Online  
DOI: 10.1039/C9TC00701F

In the device structure of organic light-emitting diodes (OLEDs), several organic materials are being used and they are hole injection material, hole transport material, electron transport material, host and emitters.<sup>1-14</sup> Except for the emitters, other materials mainly or partially play a role of carrying holes or electrons and consisted of carrier transport units.<sup>1-6, 8-10</sup> Hole carrying units are embedded in the hole injection material, hole transport material and host material, while electron carrying units are implanted in the electron transport material and host material. Therefore, many hole and electron carrying units have been explored to develop the organic materials for OLEDs.

As the hole carrying units, carbazole and aromatic amine have been popular because of efficient hole generation and transport.<sup>9, 15-18</sup> However, the carbazole is a weak hole transport unit and is not appropriate as the building unit of hole transport materials except for high triplet energy hole transport materials with triplet exciton blocking function.<sup>19</sup> The aromatic amine unit is also common as a strong hole transport unit and mostly used to build hole transport materials.<sup>18-20</sup> Other than the carbazole and aromatic amine units, indole and acridine units can also be included as the hole transport units, but they were not as popular as the carbazole and aromatic amine units.<sup>21, 22</sup> In fact, not many hole transport units are available in the design of hole transport and host materials, and more hole transport units are required to diversify the material design of host and hole transport materials.

In this work, an indole derived unit, indoloindole, was introduced as a new hole transport unit of hole transport type (p-type) host. The indoloindole was synthesized and used to develop 1,3-bis(6-phenylindolo[2,3-b]indol-5(6H)-yl)benzene (mIDIDP) host. The indoloindole derived mIDIDP functioned as a strong p-type host for yellow phosphorescent OLEDs. It was demonstrated that the indoloindole moiety performed well as the building block of the p-type host and the yellow phosphorescent OLEDs possessing an exciplex type mixed host built on the mIDIDP p-type host achieved lifetime improvement by more than 10 times compared with a common exciplex host while achieving high external quantum efficiency over 20%.

## Results and discussion

The synthetic path of the mIDIDP host derived from a new hole transport moiety is described in **Scheme 1**. Indoloindole was synthesized through 3 step synthetic process starting from 1H-indole. 1-Phenyl-1H-indole was successfully synthesized with high yield of 90% by Ullmann reaction according to literature.<sup>23</sup> Then the subsequent Heck reaction with 1-iodo-2-nitrobenzene was carried out to obtain a 3-(2-nitrophenyl)-1-phenyl-1H-indole intermediate with a synthetic yield around 60%. After that, a ring closing reaction using triphenylphosphine was carried out to prepare the new hole transport moiety, 5-phenyl-5,6-dihydroindolo[2,3-b]indole (IDID). The final product, mIDIDP, was synthesized by Ullman reaction using 1,3-diiodobenzene. After purification, mIDIDP was obtained as a pure product with a high purity over 99.9% and a synthetic yield around 60%. The mIDIDP was confirmed by analysis using <sup>1</sup>H nuclear magnetic spectrometer (NMR), <sup>13</sup>C NMR and mass spectroscopy. The details of synthetic procedure are summarized in experimental part.

The IDID moiety which has two 1H-indole units fused together was designed for strong donor character by the electron richness of the indole unit. The fusion of the two indole units may strengthen the donor character of the IDID moiety, which was estimated by examining the molecular orbital calculation results of the IDID moiety using B3LYP function and 6-31G(d) basis set. The calculation result of molecular orbital distribution of the IDID moiety is shown in **Figure 1** in comparison with that of conventional carbazole, diphenylamine, and dimethylacridine moieties. The highest occupied molecular orbital (HOMO) of the IDID moiety was well spread over the two indole moieties and was shallower than that of carbazole and diphenylamine moieties, indicating the strong donor character of the IDID moiety. It was similar to a dimethylacridine moiety in terms of donor character considering the similar HOMO level of IDID and dimethylacridine.

The electronic orbital distribution of the HOMO and LUMO of the mIDIDP host was also calculated using the B3LYP 6-31G basis set. **Figure 2** shows the HOMO and LUMO orbital distribution of mIDIDP.

The HOMO was localized on the IDID moiety of the mIDIDP because of electron richness of the IDID moiety, whereas the LUMO was observed in the phenyl linker between IDID moieties. The calculated HOMO level of the mIDIDP host was -4.88 eV, which was shallower than that of 1,3-di(9H-carbazol-9-yl)benzene (mCP) (-5.41 eV) and 1,3-bis(9,9-dimethylacridin-10(9H)-yl)benzene (mAP) (-4.90 eV). From the calculations, the mIDIDP host is expected to have stronger electron donating property than mCP and mAP.

The theoretically estimated HOMO and LUMO of the mIDIDP host were experimentally determined from the onset of oxidation and reduction scan using cyclic voltammetry. The oxidation and reduction data in **Figure 3** estimated the HOMO and LUMO as -5.64 and -2.38 eV, respectively. As expected from the calculation result, the mIDIDP showed shallower HOMO level than mCP (-6.10 eV) and mAP (-5.88 eV), supporting the insight that the fusion of the two indole units in the IDID moiety intensify the donor character of the mIDIDP host.

The photophysical behaviour of the mIDIDP host was studied using ultraviolet-visible (UV-Vis) absorption measurement and photoluminescence (PL) emission measurement (**Figure 4**). The UV-Vis absorption spectrum of mIDIDP showed  $n-\pi^*$  transition and  $\pi-\pi^*$  transition in the wavelength region of 250-370 nm. The UV-Vis absorption gap of the mIDIDP host was 3.31 eV from the onset energy of the absorption spectrum. The PL emission spectrum of mIDIDP in tetrahydrofuran solution ( $1.0 \times 10^{-5}$  M concentration) at room temperature showed a main emission peak at 369 nm corresponding to singlet energy of 3.36 eV and vibrational peaks at long wavelength. The PL spectrum at 77 K from frozen tetrahydrofuran solution with 2  $\mu$ s delay time exhibited phosphorescent emission at 492 nm corresponding to triplet energy of 2.52 eV. It can be noted from the triplet energy that the mIDIDP can be applied as the host of yellow phosphors. The triplet energy of the mIDIDP host was similar to that of the IDID moiety as shown in Figure S1. The material analysis data are summarized in **Table 1**.

Thermal properties of mIDIDP were also analysed to understand the thermal stability of mIDIDP. **Figure 5(a)** and **(b)** show differential scanning calorimeter analysis result of glass transition temperature

( $T_g$ ) and thermogravimetric analysis output of thermal decomposition temperature ( $T_d$ ) of mIDIDP. Since the host materials having low  $T_g$  can be deformed or crystallized during electrical operation of the OLEDs, they should have high  $T_g$  for stable operation. High  $T_g$  of 137.4 °C was observed in the mIDIDP host in spite of low molecular weight possibly due to the rigid IDID donor moiety. Also,  $T_d$  of mIDIDP was 467.9 °C up to 5% weight loss, describing the thermal stability of the mIDIDP host.

The mIDIDP host can be regarded as the strong hole transport type host from the HOMO level of -5.64 eV. Therefore, it was applied as the p-type host of the mixed host. It was mixed with an electron transport type host (n-type host) to develop the p-n mixed host. The n-type host for the mixed host was 2,2',2''-(1,3,5-benzinetriyl)-tris(1-phenyl-1-*H*-benzimidazole) (TPBi). Prior to device application, the mixed film of mIDIDP and TPBi was analysed by PL measurement to study the nature of the mIDIDP:TPBi mixed host. The fluorescent emission spectra of each host and mixed host are shown in **Figure 6**. The peak wavelengths of the mIDIDP, TPBi and mIDIDP:TPBi hosts were 395, 365 and 461 nm, respectively. The mIDIDP:TPBi mixed film showed broadened and red-shifted PL spectrum compared with the mIDIDP and TPBi, indicating that the mixed host of mIDIDP and TPBi is an exciplex type host as reported in other publications<sup>24-27</sup>.

In several publications, the exciplex type host could enhance external quantum efficiency (EQE) and extend operational lifetime of the phosphorescent OLEDs.<sup>24-27</sup> To evaluate the performances of the mIDIDP host as a p-type host in the mIDIDP:TPBi exciplex host, yellow phosphorescent OLEDs were fabricated using the mIDIDP:TPBi (50:50) mixed host. Iridium(III) bis(4-phenylthieno[3,2-*c*]pyridinato-N,C2')acetylacetonate (PO-01) was used as the phosphor to fabricate the phosphorescent OLEDs at a doping concentration of 5 wt%. Reference host was tris(4-carbazoyl-9-ylphenyl)amine (TCTA):TPBi (50:50) host which is well known as an exciplex host.<sup>27</sup> The details of device structure and energy diagram are summarized in supporting information (**Figure S2**). The TCTA p-type host has the HOMO/LUMO levels of -5.70/-2.40 eV, which are almost the same values as those of mIDIDP. Therefore, the comparison of the mIDIDP:TPBi and TCTA:TPBi mixed host is suitable for judging the

performance of the mIDIDP as the p-type host of the exciplex host. The device performances of the mIDIDP:TPBi and TCTA:TPBi devices are summarized in **Figure 7** and **Table 2**. In the current density (J)-voltage (V)-luminance (L) curves (**Figure 7(a)**), the mIDIDP:TPBi device showed higher J and L than the TCTA:TPBi host. Compared with the TCTA p-type host, the mIDIDP host can be considered as the strong p-type host judging from the single carrier density of the TCTA and mIDIDP hole only devices in **Figure 8**. The strong hole transport property of the mIDIDP host increased the J of the mIDIDP:TPBi mixed host device. Considering the similar HOMO level of TCTA and mIDIDP, the increase of J in the mIDIDP:TPBi device is due to the improved hole transport properties rather than hole injection properties by reduced hole injection barrier. The power efficiency-luminance plots and current efficiency-luminance plots were shown in **Figure S3** and **Figure S4**.

The EQE of the mIDIDP:TPBi device in **Figure 7(b)** was equivalent to that of the TCTA:TPBi device, describing the appropriateness of the mIDIDP host as the p-type host. The maximum EQEs of the mIDIDP:TPBi and TCTA:TPBi devices were 21.4% and 22.2%, respectively. The EQE drop at high L was insignificant by preserving the high EQE of the devices. For example, the EQE of the mIDIDP:TPBi device at 5,000 cd/m<sup>2</sup> was 20.9%, which is similar to the maximum EQE. Balance of holes and electrons along with efficient carrier injection in the mIDIDP:TPBi device enabled the small efficiency roll-off. The mIDIDP:TPBi and TCTA:TPBi hosts were comparable in terms of energy transfer because the same electroluminescence (EL) spectra were obtained in the yellow phosphorescent OLEDs (**Figure 7(c)**). The peak wavelength of the two phosphorescent OLEDs was 561 nm.

The device lifetime up to 80% of initial L at 1,000 cd/m<sup>2</sup> was also examined to evaluate the mIDIDP host as the lifetime elongating host. The lifetime measurement result of the two devices is shown in **Figure 9**. The device lifetime of the mIDIDP:TPBi (226.9 h) device was much longer than that of the TCTA:TPBi (17.1 h) device. Surprisingly, more than 10 times extension of the device lifetime was noted by replacing TCTA with mIDIDP in the exciplex host. This result showed that the mIDIDP host in the mixed host device is much better than the TCTA host as the p-type host.

To figure out the reason for the extended lifetime in the mIDIDP:TPBi device, hole carrier stability test of mIDIDP and TCTA was carried out by fabricating single carrier devices. The hole carrier stability test was performed because the p-type hosts mostly carry holes rather than electrons. The hole only device was operated at a constant  $J$  of  $7.5 \text{ mA/cm}^2$ . As a result of hole carrier stability test at a constant  $J$  condition (**Figure 10**), the driving voltage of the TCTA was significantly increased, but that of the mIDIDP device was not increased at all. As the voltage rise during electrical operation is caused by increased resistance in the organic layer or at the interface by degradation of the organic materials, it can be stated that the reason of the improved lifetime of the mIDIDP:TPBi device is the good hole carrier stability of the mIDIDP p-type host. The chemical structure merging two indole units could withstand the hole carriers during device operation.

## Conclusions

New hole type moiety, IDID, was designed and developed for good hole transport property and hole stability. The mIDIDP host derived from the IDID moiety was synthesized and applied as the p-type host with TPBi in exciplex type mixed host for yellow phosphorescent OLEDs. The PO-01 doped mIDIDP:TPBi device showed device lifetime more than 10 times longer than that of the common TCTA:TPBi device while demonstrating high EQE over 20%. This work demonstrated that the new mIDIDP host derived from IDID moiety can efficiently work as a p-type host possessing high stability against the hole carriers.

## Experimental

### General information

1H-indole, triphenylphosphine, copper iodide, and 1,10-phenanthroline were product of Sigma Aldrich Co.. Iodobenzene, 1-iodo-2-nitrobenzene, and 1,3-diiodobenzene were purchased from Alfa Aesar,

Thermo Fisher Scientific Inc.. Cesium carbonate, potassium carbonate, 1,4-dioxane, N,N-dimethylformamide (DMF), and o-dichlorobenzene (o-DCB) were supplied from Duksan Sci. Co.. View Article Online  
DOI: 10.1039/C9TC00701F

Palladium (II) acetate was purchased from P&H Tech Co. Methylene chloride (MC) and n-hexane were bought from Samchun Pure Chemical Co., Ltd.. All of purchased products were used without any purification. The  $^1\text{H}$  and  $^{13}\text{C}$  nuclear magnetic resonance (NMR) spectra of intermediate compounds and final product were measured by using AVANCE III HD (Bruker, 500 MHz) spectrometer. The mass spectroscopy of all compounds except final product was recorded with Advion, Expression<sup>L</sup> CMS spectrometer with APCI mode. The final compound analysis was proceeded with fast atom bombardment (FAB) mode measured by JMS-700 (JEOL). The absorption spectrum and emission spectrum of compound was measured by using spectrophotometer (JASCO, V-730) and fluorescence spectrophotometer (PerkinElmer, LS-55) respectively. Purity of the final compound was measured using high performance liquid chromatography (Younglin Instrument Co.) using a mobile phase of tetrahydrofuran:water (7:3).

## Synthesis

### 1-Phenyl-1H-indole

Synthetic method of 1-phenyl-1H-indole was already reported in previous literature.<sup>23</sup>

### 3-(2-Nitrophenyl)-1-phenyl-1H-indole

1-Phenyl-1H-indole (3.00 g, 15.52 mmol), 1-iodo-2-nitrobenzene (5.41 g, 21.73 mmol), potassium carbonate (6.44 g, 46.57 mmol) and palladium(II) acetate (0.17 g, 0.78 mmol) were poured into 250 ml 2-neck round-bottomed flask. Then, 1,4-dioxane (100 ml) was added into reaction mixture and then the mixture was bubbled with a nitrogen gas for 1 h. After degassing, the reaction mixture was heated to 110 °C. After 14 h, the reaction mixture was cooled down and extracted with methylene chloride. The separated organic layer was then filtered with celite/silica filter and concentrated using a rotary evaporator. A crude product was purified by column chromatography using a mixed eluent (n-hexane:

methylene chloride=1:2). After all purification, a yellow powder was obtained. (2.88 g, Yield 59%)

<sup>1</sup>H NMR (500 MHz, CDCl<sub>3</sub>) : δ 7.78 (d, 1H, J=7.00 Hz), 7.70 (d, 1H, J=7.00 Hz), 7.53 (t, 1H, J=7.50 Hz), 7.45 (d, 1H, J=7.50 Hz), 7.42 (t, 1H, J=7.75 Hz), 7.36-7.27 (m, 4H), 7.24-7.18 (m, 4H), 6.74 (s, 1H), <sup>13</sup>C NMR (125 MHz, CDCl<sub>3</sub>) : δ 149.3, 138.5, 137.3, 135.7, 133.5, 132.6, 129.5, 129.1, 128.2, 127.9, 127.5, 124.3, 123.1, 121.2, 121.0, 110.8, 104.7, MS (ASAP) m/z : Found 315.16 [(M+H)<sup>+</sup>]. Calculated For C<sub>20</sub>H<sub>14</sub>N<sub>2</sub>O<sub>2</sub> : 314.34, T<sub>m</sub>=136.6 °C

### 5-Phenyl-5,6-dihydroindolo[2,3-b]indole

3-(2-Nitrophenyl)-1-phenyl-1H-indole (2.00 g, 6.36 mmol), triphenylphosphine (5.01 g, 19.09 mmol) and o-dichlorobenzene (20 ml) were added into a round-bottomed flask and heated under reflux condition. After 24 h, the mixture was cooled down and adsorbed into a silica gel. The adsorbed crude product was purified by column chromatography using a mixed solvent (n-hexane: methylene chloride=2:1). The final product showed ivory-white after all purification. (1.25 g, Yield 70%)

<sup>1</sup>H NMR (500 MHz, DMSO) : δ 11.50 (s, 1H), 7.87 (d, 1H, J=7.00 Hz), 7.75 (d, 2H, J=7.50 Hz), 7.69 (t, 2H, J=7.75 Hz), 7.61 (d, 1H, J=8.00 Hz), 7.56 (d, 1H, J=8.50 Hz), 7.47 (t, 1H, J=7.25 Hz), 7.42 (d, 1H, J=8.00 Hz), 7.28-7.19 (m, 3H), 7.02 (t, 1H, J=7.25 Hz), <sup>13</sup>C NMR (125 MHz, DMSO) : δ 140.3, 139.9, 138.5, 130.1, 129.9, 126.4, 126.0, 125.1, 124.8, 122.7, 121.8, 119.7, 118.3, 118.2, 117.5, 115.7, 114.1, 112.5, 110.6 MS (ASAP) m/z : Found 283.09 [(M+H)<sup>+</sup>]. Calculated For C<sub>20</sub>H<sub>14</sub>N<sub>2</sub> : 282.34, T<sub>m</sub>=181.5 °C

### 1,3-Bis(6-phenylindolo[2,3-b]indol-5(6H)-yl)benzene (mIDIP)

1,3-Diiodobenzene (1.50 g, 4.55 mmol), 5-phenyl-5,6-dihydroindolo[2,3-b]indole (2.82g, 10.00 mmol), copper iodide (1.73 g, 9.10 mmol), potassium carbonate (1.89 g, 13.64 mmol) and 1,10-phenanthroline (1.64 g, 9.10 mmol) were added into a pressure tube. DMF (30 ml) was added into the pressure tube and then the pressure tube was heated to 150 °C for 12 h. After the reaction, excess amount of methylene chloride was added into the reaction mixture and the mixture was filtered with celite/silica gel. The filtrate

was then concentrated using a rotary evaporator and adsorbed into a silica gel. The crude product was purified with column chromatography using a mixed eluent (n-hexane: methylene chloride=1:1). After recrystallization, the product was sublimed with train sublimation machine several times. A white product was obtained after all purification. (1.71 g, Yield 59%)

<sup>1</sup>H NMR (500 MHz, CDCl<sub>3</sub>) : δ 8.14(s, 1H), 7.93-7.86 (m, 3H), 7.76 (d, 6H, J=7.50 Hz), 7.70 (d, 2H, J=8.00 Hz), 7.64 (t, 6H, J=6.75 Hz), 7.57 (d, 2H, J=8.00 Hz), 7.46 (t, 2H, J=7.50 Hz), 7.26 (t, 4H, J=7.75 Hz), 7.13 (t, 4H, J=7.25 Hz), <sup>13</sup>C NMR (125 MHz, CDCl<sub>3</sub>) : δ 141.1, 141.1, 140.5, 138.9, 131.0, 129.9, 127.2, 127.0, 126.7, 126.1, 124.3, 123.1, 123.0, 122.9, 120.1, 119.9, 118.8, 118.7, 116.2, 115.8, 111.2, 111.1 MS (HR-FAB) m/z Found : 638.2468 [(M+H)<sup>+</sup>]. Calculated For C<sub>46</sub>H<sub>30</sub>N<sub>4</sub> : 638.7572, T<sub>m</sub>=263.1 °C

### Device Fabrication and measurements

Patterned ITO substrates were used for all devices fabrication. Organic materials, LiF and Al were deposited at a high pressure of  $1.0 \times 10^{-6}$  torr.

The device structure is described below.

ITO (50 nm)/ DNTPD (60 nm)/ BPBPA (20 nm)/ PCZAC (10 nm)/ emitting layer (30 nm)/ DBFTrz (5 nm)/ ZADN (30 nm)/ LiF (1.5 nm)/ Al (200 nm)

N<sup>4</sup>,N<sup>4'</sup>-Bis[4-[bis(3-methylphenyl)amino]phenyl]-N<sup>4</sup>,N<sup>4'</sup>-diphenyl-[1,1'-biphenyl]-4,4'-diamine (DNTPD) and N,N,N',N'-tetra[(1,10-biphenyl)-4-yl]-(1,10-biphenyl)-4,4'-diamine (BPBPA) were used as a hole injection layer and a hole transport layer, respectively. The 9,9-dimethyl-10-(9-phenyl-9H-carbazol-3-yl)-9,10-dihydroacridine (PCZAC) was deposited on BPBPA and used as an exciton blocking layer. 2,8-Bis(4,6-diphenyl-1,3,5-triazin-2-yl)dibenzo[b,d]furan (DBFTrz) and 9,10-di(naphthalene-2-yl)anthracen-2-yl-(4,1-phenylene)(1-phenyl-1Hbenzo[d]imidazole (ZADN) were used as an exciton blocking layer and an electron transport layer, respectively. The hosts of the emission layer were either mIDIDP:TPBi or TCTA:TPBi. The doping concentration of PO-01 was fixed with 5 wt% in all devices.

The single charge device structure is summarized below.

ITO (50 nm)/ PEDOT:PSS (60 nm)/ mIDIDP or TCTA (50 nm)/ Al (200 nm)

The fabricated devices were analyzed using Keithley 2400 source measurement unit and CS 2000 spectroradiometer at room temperature after encapsulation.

View Article Online  
DOI: 10.1039/C9TC00701F

#### Acknowledgements

This work was supported by Basic Science Research Program (2016R1A2B3008845) and Nano Materials Research Program (2016M3A7B4909243) through the National Research Foundation of Korea funded by Ministry of Science, ICT and Future Planning.

## References

View Article Online  
DOI: 10.1039/C9TC00701F

1. U. Mitschke and P. Bauerle, *J. Mater. Chem.*, 2000, **10**, 1471-1507.
2. L. S. Hung and C. H. Chen, *Mater. Sci. Eng. R Rep.*, 2002, **39**, 143-222.
3. A. P. Kulkarni, C. J. Tonzola, A. Babel and S. A. Jenekhe, *Chem. Mater.*, 2004, **16**, 4556-4573.
4. S. O. Jeon, S. E. Jang, H. S. Son and J. Y. Lee, *Adv. Mater.*, 2011, **23**, 1436-1441.
5. Y. T. Tao, C. L. Yang and J. G. Qin, *Chem. Soc. Rev.*, 2011, **40**, 2943-2970.
6. S. M. Kim, J. H. Yun, S. Y. Byeon, S. K. Jeon, J. Y. Lee, *J. Ind. Eng. Chem.*, 2017, **51**, 295.
7. C. Adachi, M. A. Baldo, M. E. Thompson and S. R. Forrest, *J. Appl. Phys.*, 2001, **90**, 5048-5051.
8. Y. Shirota and H. Kageyama, *Chem. Rev.*, 2007, **107**, 953-1010.
9. S. O. Jeon, K. S. Yook, C. W. Joo and J. Y. Lee, *Adv. Funct. Mater.*, 2009, **19**, 3644-3649.
10. Y. Im, S. H. Han, J. Y. Lee, *J. Ind. Eng. Chem.*, 2018, **66**, 381.
11. Q. S. Zhang, B. Li, S. P. Huang, H. Nomura, H. Tanaka and C. Adachi, *Nat. Photonics*, 2014, **8**, 326-332.
12. M. Kim, S. K. Jeon, S. H. Hwang and J. Y. Lee, *Adv. Mater.*, 2015, **27**, 2515-2520.
13. D. R. Lee, B. S. Kim, C. W. Lee, Y. Im, K. S. Yook, S. H. Hwang and J. Y. Lee, *ACS Appl. Mater. Interfaces*, 2015, **7**, 9625-9629.
14. Y. Im, S. Y. Byun, J. H. Kim, D. R. Lee, C. S. Oh, K. S. Yook and J. Y. Lee, *Adv. Funct. Mater.*, 2017, **27**.
15. P. Kundu, K. R. J. Thomas, J. T. Lin, Y. T. Tao and C. H. Chien, *Adv. Funct. Mater.*, 2003, **13**, 445-452.
16. K. Brunner, A. van Dijken, H. Borner, J. Bastiaansen, N. M. M. Kiggen and B. M. W. Langeveld, *J. Am. Chem. Soc.*, 2004, **126**, 6035-6042.

17. M. H. Tsai, H. W. Lin, H. C. Su, T. H. Ke, C. C. Wu, F. C. Fang, Y. L. Liao, K. T. Wong and C. I. Wu, *Adv. Mater.*, 2006, **18**, 1216-1220. View Article Online  
DOI: 10.1039/C9TC00701F
18. M. Y. Lai, C. H. Chen, W. S. Huang, J. T. Lin, T. H. Ke, L. Y. Chen, M. H. Tsai and C. C. Wu, *Angew. Chem.*, 2008, **47**, 581-585.
19. I. Y. Wu, J. T. Lin, Y. T. Tao, E. Balasubramaniam, Y. Z. Su and C. W. Ko, *Chem. Mater.*, 2001, **13**, 2626-2631.
20. Y. J. Cho, O. Y. Kim and J. Y. Lee, *Org. Electron.*, 2012, **13**, 351-355.
21. X. Y. Liu, F. Liang, L. Ding, Q. Li, Z. Q. Jiang and L. S. Liao, *Dyes Pigm.*, 2016, **126**, 131-137.
22. H. Tsuji, Y. Yokoi, C. Mitsui, L. Ilies, Y. Sato and E. Nakamura, *Chem. Asian J.*, 2009, **4**, 655-657.
23. J. B. Ernst, A. Ruhling, B. Wibbeling and F. Glorius, *Chem. Eur. J.*, 2016, **22**, 4400-4404.
24. M. E. Kondakova, T. D. Pawlik, R. H. Young, D. J. Giesen, D. Y. Kondakov, C. T. Brown, J. C. Deaton, J. R. Lenhard and K. P. Klubek, *J. Appl. Phys.*, 2008, **104**.
25. Y. S. Park, S. Lee, K. H. Kim, S. Y. Kim, J. H. Lee and J. J. Kim, *Adv. Funct. Mater.*, 2013, **23**, 4914-4920.
26. S. K. Shin, S. H. Han and J. Y. Lee, *J. Mater. Chem. C*, 2018, **6**, 10308-10314.
27. W. Song and J. Y. Lee, *Org. Electron.*, 2017, **48**, 285-290.

**List of Table****Table 1.** Material property data of mIDIDP[View Article Online](#)  
DOI: 10.1039/C9TC00701F**Table 2.** Device performance of mixed host devices

**Table 1.** Material property data of mIDIDP

	<b>E<sub>HOMO</sub></b> (eV)	<b>E<sub>LUMO</sub></b> (eV)	<b>E<sub>gap</sub></b> (eV)	<b>E<sub>UV-gap</sub></b> (eV)	<b>E<sub>s</sub></b> (eV)	<b>E<sub>T</sub></b> (eV)	<b>T<sub>g</sub></b> (°C)	<b>T<sub>d</sub></b> (°C)
<b>mIDIDP</b>	-5.64	-2.38	3.26	3.31	3.36	2.52	137.4	467.9

View Article Online  
DOI: 10.1039/C9TC00701F

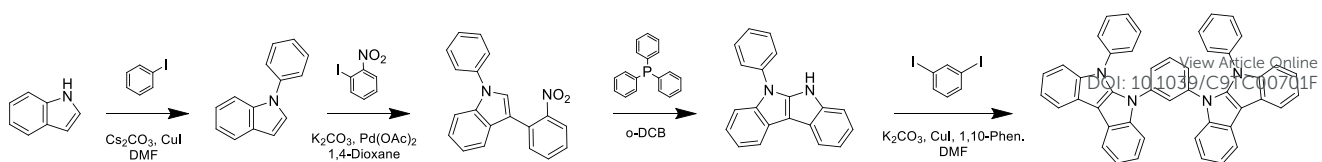
**Table 2.** Device performance of mixed host devices

	<b>V<sub>d</sub></b> <b>(V)</b>	<b>I</b> <b>(mA/cm<sup>2</sup>)</b>	<b>CIE</b>	<b>QE(%)</b>		<b>PE(lm/W)</b>		<b>CE(Cd/A)</b>		<b>LT<sub>80</sub></b> <b>(h)</b>
				<b>[5000cd/m<sup>2</sup>]</b>	<b>[Max]</b>	<b>[5000cd/m<sup>2</sup>]</b>	<b>[Max]</b>	<b>[5000cd/m<sup>2</sup>]</b>	<b>[Max]</b>	
mIDIDP: TPBi	5.6	7.4	(0.49, 0.51)	20.9	21.4	37.8	52.4	67.7	70.1	226.9
TCTA: TPBi	5.7	7.2	(0.49, 0.51)	21.5	22.2	38.2	52.4	69.6	71.9	17.1

\*All data was measured at 5,000 cd/m<sup>2</sup>

\*\*QE=Quantum Efficiency, PE=Power Efficiency, CE=Current Efficiency, V<sub>d</sub>=Driving voltage

**List of figures**View Article Online  
DOI: 10.1039/C9TC00701F**Scheme 1.** Synthetic method for mIDIDP**Figure 1.** Calculation data of moieties**Figure 2.** Orbital distribution of mIDIDP host**Figure 3.** CV measurement of mIDIDP**Figure 4.** Uv-Vis absorption spectrum and PL emission spectra of mIDIDP**Figure 5.** Thermal property analysis of mIDIDP host with (a) DSC and (b) TGA**Figure 6.** PL emission spectra of mIDIDP, TPBi and mixed film**Figure 7.** (a) J-V-L curves, (b) EQE-L curves, (c) electroluminescence spectra of mixed host devices**Figure 8.** J-V curves of single charge device**Figure 9.** Luminance-lifetime plots of devices**Figure 10.** hole stability test of single charge device



**Scheme 1.** Synthetic method for mIDIDP

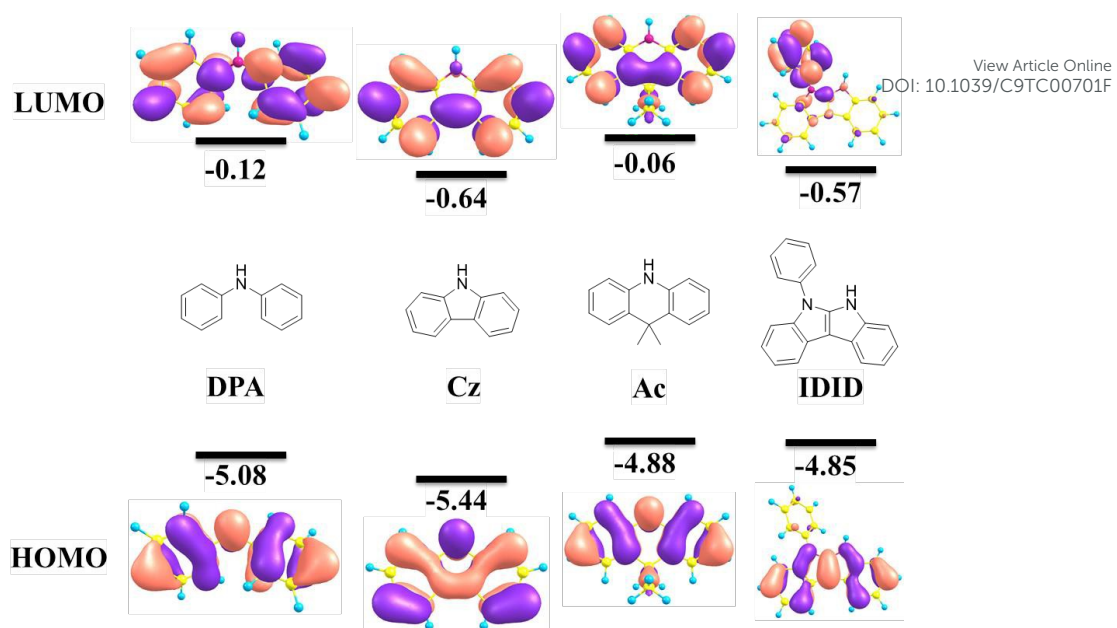
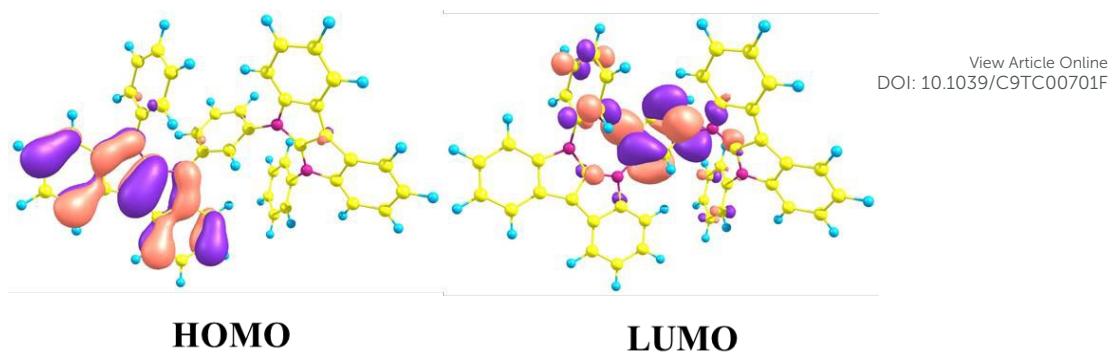
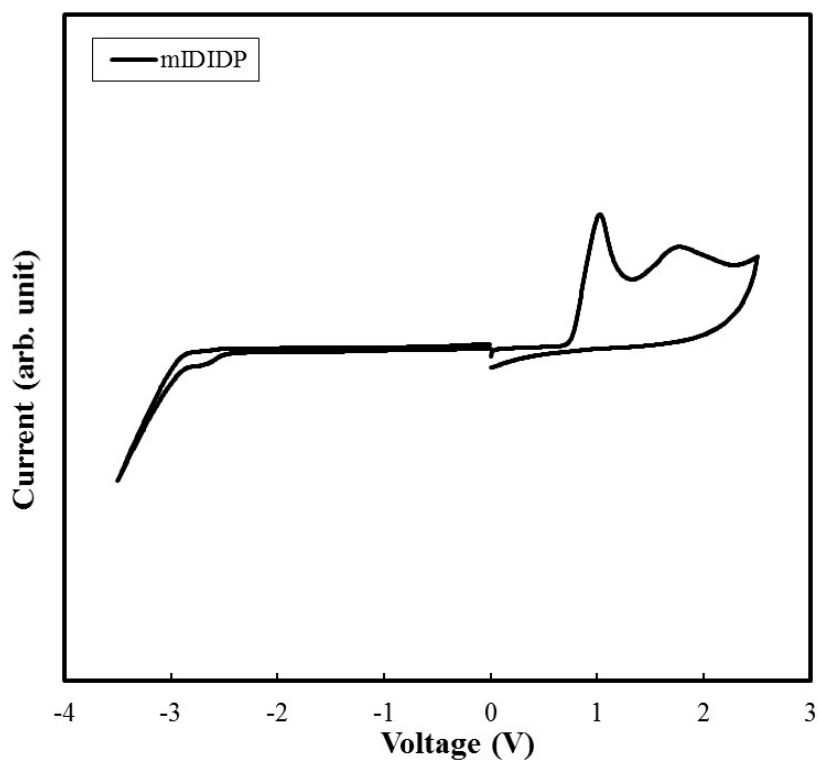


Figure 1. Calculation data of moieties



**Figure 2.** Orbital distribution of mIDIDP host



View Article Online  
DOI: 10.1039/C9TC00701F

**Figure 3.** CV measurement of mIDIDP

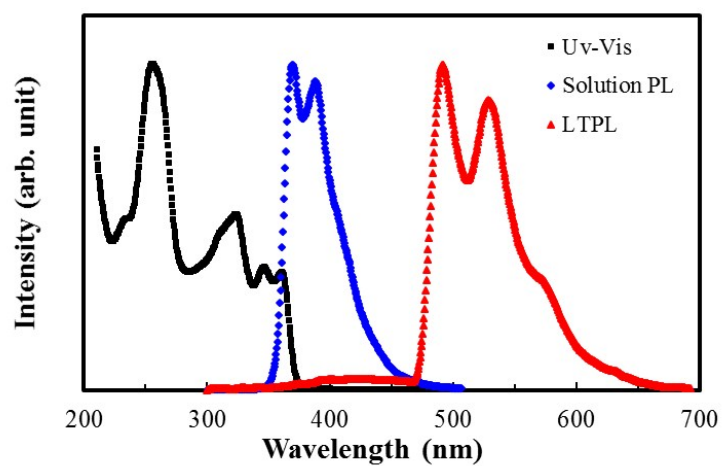


**Figure 4.** Uv-Vis absorption spectrum and PL emission spectra of mIDIDP

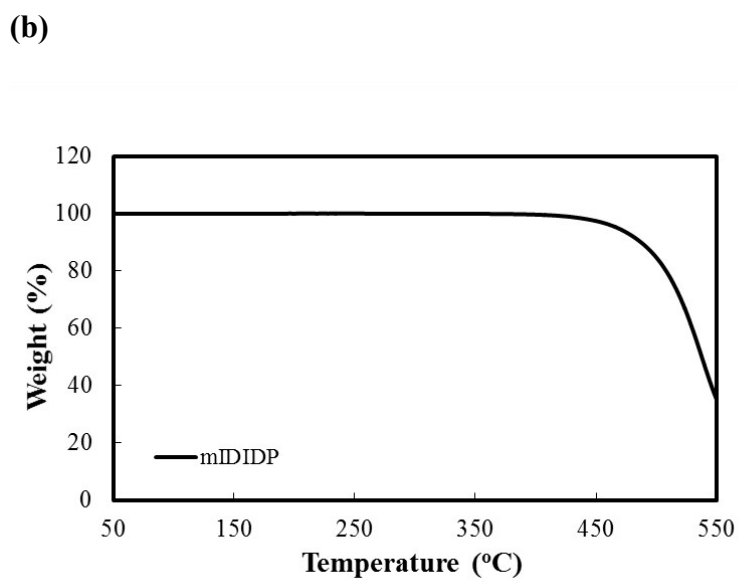
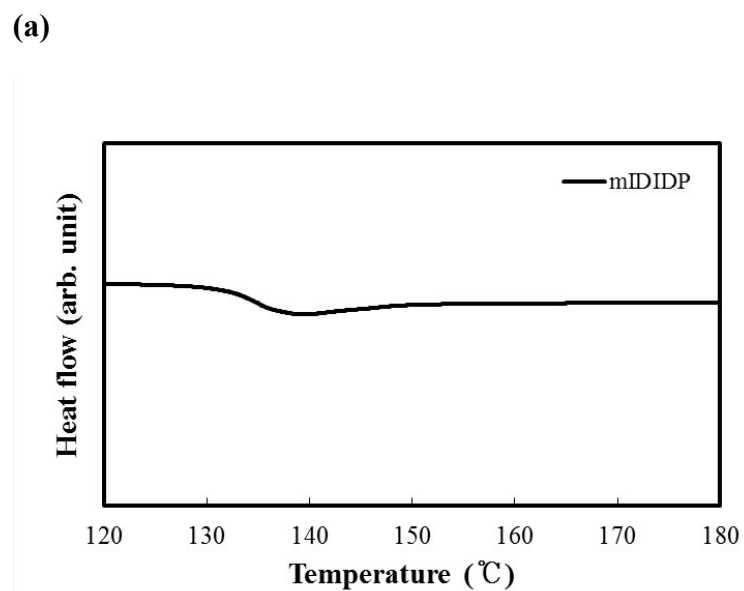
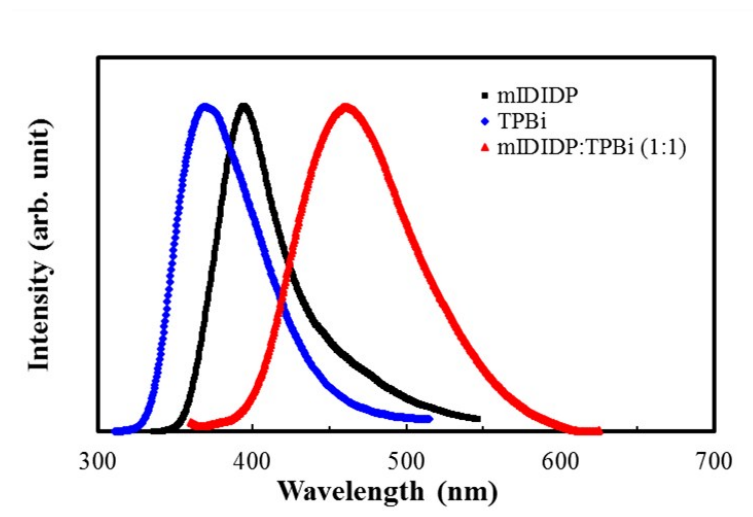


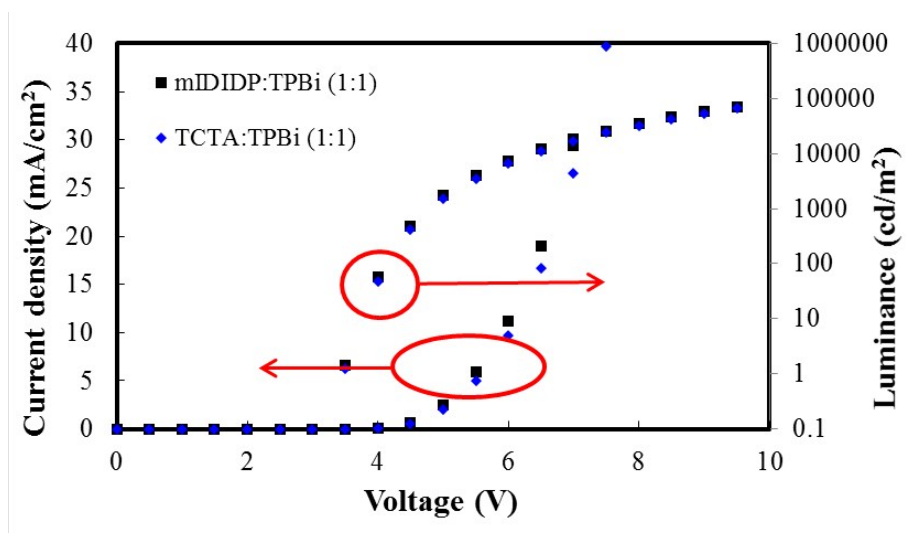
**Figure 5.** Thermal property analysis of mIDIDP host with (a) DSC and (b) TGA



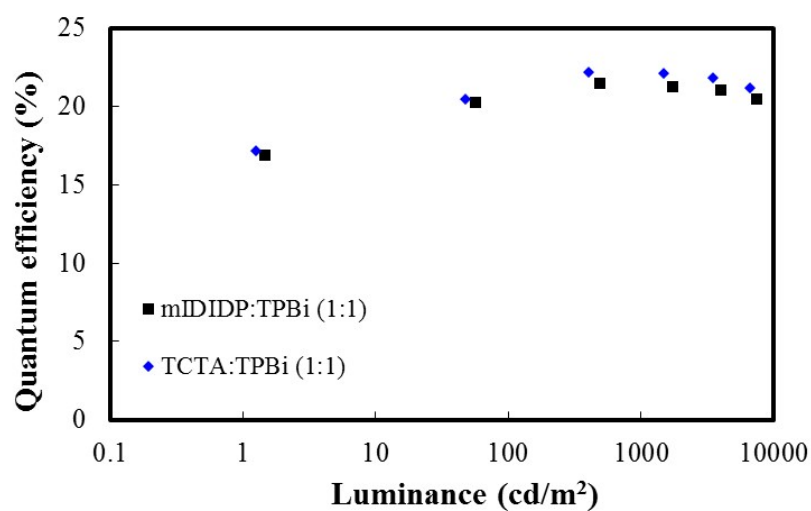
View Article Online  
DOI: 10.1039/C9TC00701F

**Figure 6.** PL emission spectra of mIDIDP, TPBi and mixed film

(a)

View Article Online  
DOI: 10.1039/C9TC00701F

(b)



(c)

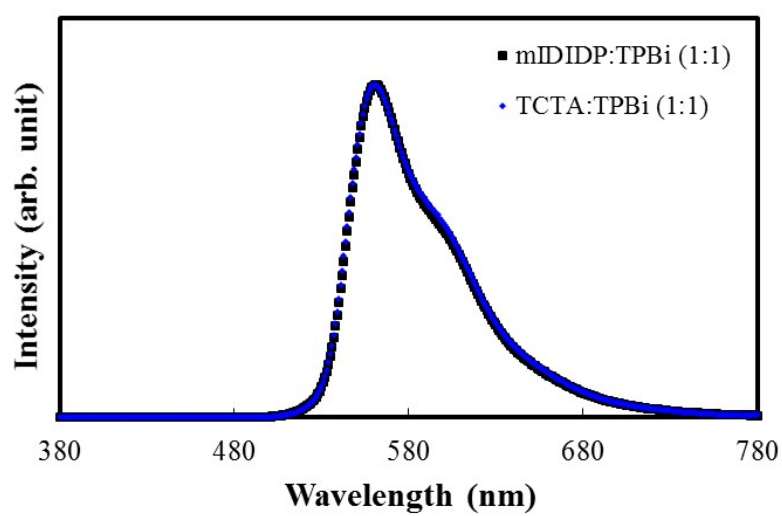
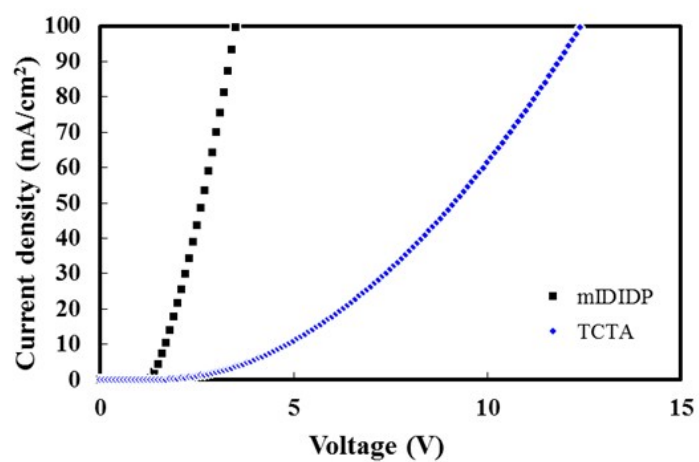
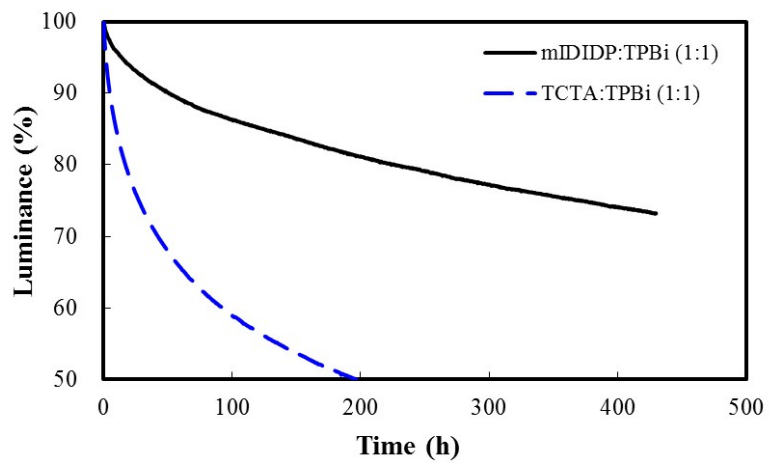


Figure 7. (a) J-V-L curves, (b) EQE-L curves, (c) electroluminescence spectra of mixed host devices



View Article Online  
DOI: 10.1039/C9TC00701F

**Figure 8.** J-V curves of single charge device



**Figure 9.** Luminance-lifetime plots of devices

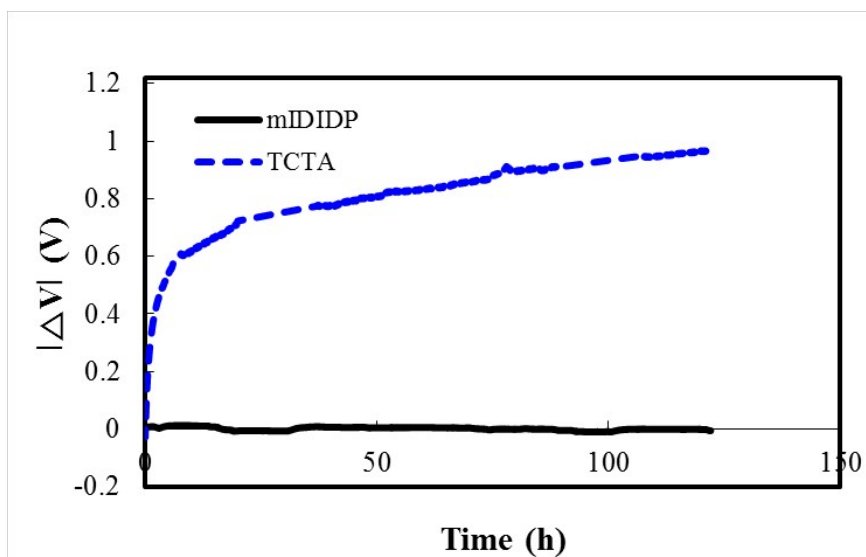


**Figure 10.** hole stability test of single charge device